Scaling frequency of channel-forming flows in snowmelt-dominated streams

Catalina Segura[1,2] and John Pitlick[1]

Received 30 June 2009; revised 22 January 2010; accepted 5 February 2010; published 29 June 2010.

[1] The scaling properties of channel-forming flows are investigated using a regional flow frequency model developed for snowmelt-dominated streams in Colorado. The model is derived from analyses of daily flow records at 32 gauging stations where we have independent measurements of the bankfull discharge. The study sites are located in alpine/subalpine basins with drainage areas ranging from 4 to 3700 km^2. The frequency distribution of daily flows at these locations can be reproduced with a broken power law (BPL) function described by two free parameters. Both parameters are strongly correlated with drainage area, and based on these correlations, a regional model capable of predicting the frequency of daily flows above the mean annual flow was formulated. The applicability of the model was tested using daily flow records from 32 similar-size basins in Idaho. The frequency distributions of daily flows in snowmelt-dominated streams in Colorado and Idaho with highly predictable hydrographs (i.e., 1 year autocorrelation above 0.7) are well fitted by the BPL function. According to the model, the frequency of flows greater than bankfull decreases downstream from about 15 d/yr in headwater reaches to about 6 d/yr in downstream reaches. These results imply that the basin response to precipitation and runoff is nonlinear. This multiscaling behavior can be physically interpreted as the result of scale-dependent variations in runoff and sediment supply, which influence downstream trends in the bankfull channel geometry and intensity of sediment transport.

Citation: Segura, C., and J. Pitlick (2010), Scaling frequency of channel-forming flows in snowmelt-dominated streams, *Water Resour. Res.*, *46*, W06524, doi:10.1029/2009WR008336.

1. Introduction

[2] Bankfull discharge is an important index of fluvial-hydraulic processes in alluvial channels. At these flow levels, water is beginning to spill onto the floodplain; thus, bankfull discharge represents the point of incipient flooding [*Williams*, 1978]. In addition, flows at or near bankfull can generate sufficient shear stress to entrain sediment from the bed and banks; hence, the bankfull discharge is described as the channel-forming flow [*Richards*, 1982]; other terms, such as the dominant discharge [*Knighton*, 1998], or the discharge that is most effective for channel maintenance [*Dunne and Leopold*, 1978], are used synonymously. However, it is now recognized that alluvial channels are formed and maintained by a range of flows with different frequencies and that single-valued indices of channel-forming processes provide only part of the information needed to quantify sediment or water quality loads or to assess processes such as nutrient retention and habitat maintenance.

[3] In streams that are gauged, the frequency of bankfull discharge can be determined directly from statistical analyses of the gauge record of peak flows or daily flows. Results from peak-flow frequency analyses of streams in a wide range of hydroclimatic settings indicate that the recurrence interval of bankfull discharge typically falls in the range of 1–3 years on the annual series [*Wolman and Leopold*, 1957; *Wolman and Miller*, 1960; *Emmett*, 1975; *Whiting et al.*, 1999; *Castro and Jackson*, 2001; *Chaplin*, 2005; *Dodov and Foufoula-Georgiou,* 2005; *Keaton et al.*, 2005; *Sherwood and Huitger,* 2005; *Mulvihill et al.*, 2009; *Rachol and Boley-Morse*, 2009]. Exceptions to this "rule of thumb" have been noted in several studies, notably those of *Williams* [1978], *Pickup and Warner* [1976], and *DeRose et al.* [2008]. Fewer studies have examined the duration of bankfull flow, expressed as the percentage of time that this discharge is equaled or exceeded. Here, there appears to be a much wider range in reported values. Empirical relations developed for gravel bed channels in Colorado and Idaho suggest that the duration of the bankfull discharge varies from ~0.4 to 24 d/yr [*Andrews*, 1984; *Pitlick and Van Steeter*, 1998; *Whiting et al.*, 1999; *Torizzo and Pitlick,* 2004]. *Dodov and Foufoula-Georgiou* [2005] examined links between channel geometry and flow frequency using data from dozens of gauging stations in the midwestern U. S. A. and found that the exceedance frequency of bankfull discharge increased systematically downstream, from about 0.3 d/yr in channels draining headwater basins (<10^2 km^2) to about 7 d/yr in channels draining larger areas (>10^4 km^2). Whereas the results presented by *Torizzo and Pitlick* [2004] and *Whiting et al.* [1999] showed no clear relation between

[1]Department of Geography, University of Colorado at Boulder, Boulder, Colorado, USA.
[2]Now at Department of Forestry and Environmental Resources, North Carolina State University, Raleigh, North Carolina, USA.

0043-1397/10/2009WR008336

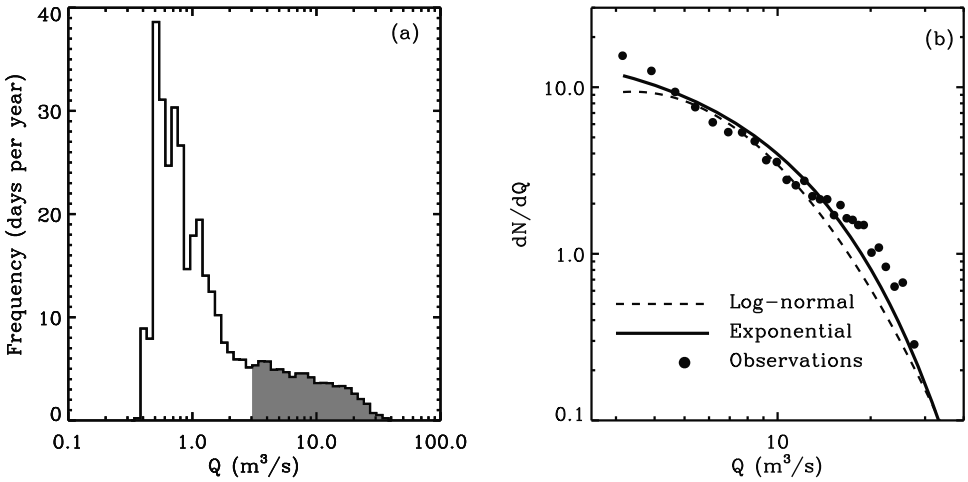

Figure 1. Frequency of daily flows of the Williams Fork River, Colo, USGS station 09036000. (a) Panel shows a histogram of daily flows; the shaded area corresponds to the range of flows analyzed in this paper. (b) Panel shows the observed frequency of daily flows and corresponding fits of the lognormal and exponential probability density functions. Figure 1b shows the frequency with which a flow range is observed is given by the integral of dN/dQ. Therefore, the y-axis (dN/dQ) has units of d $yr^{-1}Q^{-1}$.

bankfull discharge duration and drainage basin area, the results presented by *Dodov and Foufoula-Georgiou* [2005] suggest that streamflow statistics may be strongly influenced by scale-dependent changes in channel geometry and morphology.

[4] In this paper we develop a regional model to investigate the scaling properties of channel-forming flows in streams and rivers in Colorado where we have independent measurements of the bankfull discharge, Q_{bf}. The first section of the paper focuses on the development and performance of three candidate functions for fitting the distribution of daily flows in snowmelt-dominated streams. We then seek scaling relations between the parameters of the preferred distribution function and selected drainage basin characteristics, with the goal of establishing a regional model to predict the distribution of daily flows at ungauged sites. Similar to the study by *Fennessey and Vogel* [1990], we focus on the distribution of flows above the mean annual flow, Q_{ma}, which carry 80% of the annual discharge and nearly all of the bed load in gravel bed channels [*Andrews*, 1994; *Whiting et al.*, 1999; *Torizzo and Pitlick*, 2004; *Mueller and Pitlick*, 2005]. The regional model is then tested using corresponding data from similar-size streams and rivers in Idaho. The remainder of the paper focuses on scale-dependent variations in model parameters and analysis of suggested links between flow frequency and downstream trends in runoff and channel geometry.

2. Characterization of the Distribution of Daily Flows

[5] The approach commonly used for formulating daily flow frequency distributions at ungauged locations is to first identify a function that describes the frequency of flows at gauged locations, then develop a scaling relation based on drainage basin characteristics to transfer the function to ungauged locations. The extension of flow records from gauged to ungauged sites is straightforward in cases where the observed distribution has a simple statistical form, and the parameters of that distribution scale linearly over a range of drainage areas. However, frequency distributions of daily flows are often complex (e.g., bimodal) and potentially difficult to model with a simple function. *Vogel and Fennessey* [1995] note that daily streamflows originate from highly skewed populations, and sample estimates of distribution parameters may contain large bias even for sites with very long records. A number of different statistical functions have been used to model daily flow distributions, including the lognormal, exponential, γ, and pareto [*Fennessey and Vogel*, 1990; *Vogel and Fennessey*, 1993; *Nash*, 1994; *Potter*, 2001; *Vogel et al.*, 2003; *Castellarin et al.*, 2004; *Goodwin*, 2004; *Doyle et al.*, 2005; *Mueller and Pitlick*, 2005; *Archfield et al.*, 2007; *Doyle and Shields*, 2008]. The procedure for fitting these distributions is straightforward, and any one of them might offer a reasonably good fit to a series of observations. However, in our experience, none of these conventional distributions appears to fit the distribution of daily flows in snowmelt-dominated streams particularly well. Figure 1 shows the frequency distribution of daily flows for the Williams Fork River, Colo (U.S. Geological Survey [USGS] gauge 09036000), for which 73 years of record are available. Figure 1a shows that the distribution is strongly skewed and there are two modes, one reflecting base flows, the other reflecting snowmelt flows. In this case it would be difficult to model the entire distribution with a single function. Figure 1b presents a subset of the distribution with the frequencies normalized by the bin size and plotted with logarithmic scales to emphasize the behavior of intermediate to high flows. Figure 1b also shows the fit of the lognormal and the exponential functions. Unfortunately, neither of these functions fit the data particularly well. The lognormal function provides a poor fit across the entire range of flows. The exponential function provides a better fit to intermediate flows, but it underestimates both high and low flows. The observed flow distribution appears to fall as a straight line in the log-log plot, suggesting a power law behavior [*Newman,* 2005], but at a

Table 1. Hydrologic Characteristics of the Selected Streams in Colorado, Length of Record Available, and Mean Basin Elevation, from *Richter et al.* [1984][a]

USGS Gauge Number	Name	n (years)	DA (km^2)	Q_{bf} (m^3/s)	BE (m)	$d.f.$	χ^2			χ^2_ν			a_0	a_1	R(1y)
							LN	EXP	BPL	LN	EXP	BPL			
06614800	Michigan River	33	4.0	0.70[b]	3444	21	69.7	50.8	41.7	3.32	2.4	2.0	35.2	0.7	0.77
06721500	North Saint Vrain	16	84.0	11.6[c]		32	24.2	18.4	15.5	0.76	0.6	0.5	57.5	8.8	0.87
06725500	Middle Boulder Creek	87	93.8	9.50[d]	3170	34	108.4	90.8	30.3	3.19	2.7	0.9	52.5	9.5	0.82
07083000	Halfmoon Creek	60	61.1	7.00[c]	3597	31	72.2	29.5	25.4	2.33	1.0	0.8	49.4	5.3	0.79
07086500	Clear Creek	49	174	23.6[c]	3597	26	52.5	20.8	28.5	2.02	0.8	1.1	46.4	12.6	0.73
09010500	Colorado River	53	138	14.3[c]	3231	40	77.9	43.8	28.6	1.95	1.1	0.7	36.3	14.9	0.74
09022000	Fraser River	27	27.2	2.69[b]		25	64.4	43.0	28.0	2.58	1.7	1.1	43.0	2.7	0.81
09035700	Williams Fork	41	90.6	10.5[c]	3444	38	70.2	48.5	18.8	1.85	1.3	0.5	33.1	9.8	0.77
09035800	Darling Creek	41	22.7	1.83[d]	3292	28	43.6	25.3	29.9	1.56	0.9	1.1	36.3	2.0	0.79
09035900	South Williams Fork	41	70.3	7.00[c]	3322	35	55.6	29.9	18.6	1.59	0.9	0.5	41.1	6.5	0.83
09036000	Williams Fork	73	231	20.1[c]	3322	36	108.4	58.2	40.9	3.01	1.6	1.1	38.6	21.4	0.78
09047500	Snake River	58	149	12.1[d]	3475	33	88.9	38.3	37.1	2.70	1.2	1.1	47.1	11.5	0.78
09052400	Boulder Creek	28	22.2	1.12[d]	3444	30	73.7	53.1	27.9	2.46	1.8	0.9	47.9	3.1	0.83
09055300	Cataract Creek	28	31.1	1.41[d]	3292	31	45.8	33.5	20.8	1.48	1.1	0.7	39.2	4.6	0.80
09058500	Piney River	48	33.7	2.43[d]	3322	28	95.0	68.8	24.6	3.39	2.5	0.9	40.4	5.3	0.76
09058800	East Meadow Creek	40	9.4	0.58[d]	3139	26	136.0	104.9	82.9	5.23	4.0	3.2	29.3	1.1	0.76
09060500	Rock Creek	28	123	6.20[c]	2865	32	59.5	42.4	21.0	1.86	1.3	0.7	32.1	8.1	0.72
09063200	Wearyman Creek	42	22.7	0.84[d]	3322	31	56.7	42.3	48.1	1.83	1.4	1.6	34.1	2.0	0.79
09063400	Turkey Creek	43	61.6	2.69[d]	3292	30	38.6	19.3	22.4	1.29	0.6	0.7	35.2	5.1	0.77
09066000	Black Gore Creek	52	32.6	3.29[d]	3292	36	77.8	47.6	15.8	2.16	1.3	0.4	30.7	4.7	0.78
09066100	Big Horn Creek	43	11.8	1.04[d]	3383	28	68.3	38.2	23.6	2.44	1.4	0.8	40.4	2.1	0.78
09066150	Pitkin Creek	40	13.8	2.44[d]	3353	18	59.4	35.6	31.8	3.30	2.0	1.8	41.7	2.3	0.76
09066200	Booth Creek	42	15.6	3.27[d]	3322	28	66.9	35.8	19.6	2.39	1.3	0.7	36.3	2.9	0.76
09066400	Red Sandstone Creek	43	19.0	3.22[d]	3261	26	70.6	38.9	16.6	2.71	1.5	0.6	30.2	2.5	0.75
09074800	Castle Creek	25	83.4	4.45[d]	3505	34	34.6	15.0	17.6	1.02	0.4	0.5	51.7	7.0	0.85
09078100	N Fork Fryingpan River	17	31.1	3.17[b]	3475	32	29.4	20.2	11.4	0.92	0.6	0.4	35.8	4.8	0.73
09078200	Cunningham Creek	17	18.4	2.52[b]	3261	31	31.7	24.3	22.7	1.02	0.8	0.7	27.5	3.0	0.73
09081600	Crystal River	51	433	49.0[b]	3109	33	105.0	90.5	34.0	3.18	2.7	1.0	46.4	52.9	0.80
09112500	East River	84	749	37.5[b]	3109	30	118.3	80.4	27.4	3.94	2.7	0.9	47.1	59.5	0.79
09124500	Lake Fork	69	865	42.0[b]	3322	41	104.8	47.5	28.4	2.56	1.2	0.7	50.1	40.8	0.79
09242500	Elk River	36	1075	101[b]	2560	38	47.8	51.5	33.4	1.26	1.4	0.9	46.4	105.9	0.84
09244410	Yampa River	21	3700	167[b]	2621	31	37.4	42.2	28.9	1.21	1.4	0.9	44.3	209.7	0.82

[a] n, length of record available; BE, Mean Basin Elevation; $d.f.$, degrees of freedom; χ^2 and reduced χ^2 (χ^2_ν) of the fits of the lognormal (LN), exponential (EXP), and broken power law (BPL) functions to the daily flow distribution, parameters, a_0 and a_1, of the fit of the broken power law function, and annual autocorrelation (R(1y)) of daily flows.
[b] Reference for Q_{bf}: *Andrews* [1984].
[c] Reference for Q_{bf}: *Torizzo and Pitlick* [2004].
[d] Reference for Q_{bf}: *Surian and Andrews* [1999].

discharge of approximately 20 m^3/s, there is an inflection in the distribution and the slope appears to steepen.

2.1. Distribution Functions

[6] In this section we introduce three probability density functions for characterizing the distribution of daily flows in snowmelt-dominated streams. The first two functions, the lognormal (LN) and the exponential (EXP), have been used previously to model the distribution of flows within a specific range, such as flows below the median discharge [*Fennessey and Vogel*, 1990], or flows above one half the bankfull discharge [*Mueller and Pitlick*, 2005]. The third function is termed the broken power law (BPL). To our knowledge, this function has not been used to characterize statistical distributions in hydrology; however, it has been used in other disciplines to interpret transitions (breaks) in power law behavior above some characteristic scale. This transition is reflected by a break in slope of logarithmic plots of event frequency versus event size [*Newman*, 2005], giving a continuous distribution with two separate straight-line segments. The inflection in the distribution suggests that the data either do not follow a power law or that there is an upper limit to the size of events [*Burroughs and Tebbens*, 2001; *Aban et al.*, 2006].

[7] The lognormal probability density function is

$$\frac{dN}{dQ} = \frac{1}{Q\sigma\sqrt{2\pi}} \exp\left[-\frac{(\ln(Q)-\mu)^2}{2\sigma^2}\right], \quad (1)$$

where N is the number of days per year, Q is the discharge, and μ and σ are location and scale parameters, respectively. These two parameters correspond to the mean and the standard deviation of the natural logarithm of Q when the whole range of flows is considered.

[8] The exponential probability density function is

$$\frac{dN}{dQ} = b_0 e^{-b_1 Q}, \quad (2)$$

where b_0 is a normalization parameter and b_1 is the slope of the discharge-frequency relation. This distribution is simple, but as mentioned above, it fails to reproduce the frequency distribution of low and high flows in some cases.

[9] The broken power law probability density function is

$$\frac{dN}{dQ} = \frac{a_0/a_1}{(Q/a_1)^\alpha + (Q/a_1)^\beta}, \quad (3)$$

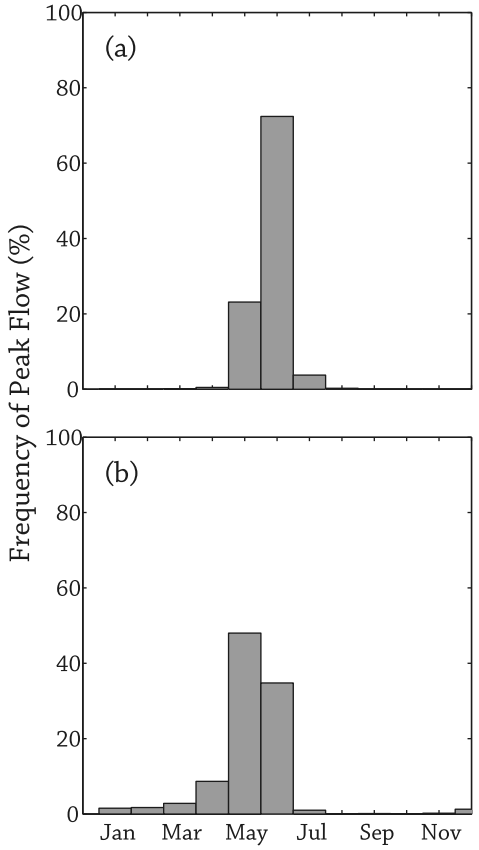

Figure 2. Seasonal distributions of peak flows at (a) 32 sites in Colorado and (b) 32 sites in Idaho.

where a_0 is a normalization parameter, a_1 is the value of Q corresponding to the inflection point of the distribution, and α and β are parameters that set the slopes of the two separate segments of the frequency distribution formed by intermediate to high flows. It is within this range of flows that we see a distinct change in the shape of the frequency distribution, which presumably reflects an upper bound on the intensity of runoff produced in alpine-subalpine basins.

2.2. Data Sources

[10] Thirty-two high-elevation basins in Colorado were selected for this analysis. These basins are located in the southern Rocky Mountains, with drainage areas ranging from 4 to 3700 km^2 (Table 1). The watersheds are generally forested with vegetation dominated by Engleman spruce (*Picea engelmannii*), subalpine fir (*Abies lasiocarpa*), and lodgepole pine (*Pinus contorta*). Most of the basins have been glaciated, and glacial deposits are found down to about 2400 m in elevation [*Surian and Andrews*, 1999]. At least 60% of the annual precipitation in the region falls as snow during the winter and spring months [*Serreze et al.*, 1999]. Peak flows in high-elevation basins in Colorado are generated almost exclusively by snowmelt (Figure 2). Rainfall from convective storms can generate significant peaks at lower elevations (<2300 m); however, our analysis is restricted to drainage basins with mean elevations above 2500 m (Table 1) where runoff from convective storms is much lower than the peaks produced by snowmelt [*Jarrett and Costa*, 1988; *Jarrett*, 1990; *Pitlick*, 1994]. The study sites were selected on the basis of four criteria: (1) minimum flow regulation, (2) daily flow records longer than 16 complete water years, (3) availability of data regarding bankfull discharge, Q_{bf}, and (4) a wide range of drainage areas (Table 1).

[11] The bankfull discharge for each site in Colorado was estimated on the basis of field surveys of channel geometry and water-surface elevation taken over a range of flows. In general, the bankfull flow level could be identified in the field by a distinct break in slope between the channel and the floodplain and by changes in vegetation. Site surveys were conducted by different investigators; however, the methods used in estimating bankfull discharges were similar. *Andrews* [1984] and *Surian and Andrews* [1999] surveyed cross sections and bankfull elevations through each of their study reaches and correlated those measurements with the observed stage-discharge relation for the gauging station. *Torizzo and Pitlick* [2004] surveyed 9–12 cross sections at each of their study sites and estimated bankfull discharge by direct observation and correlation with gauging station records. *Segura* [2008] surveyed 13–18 cross sections at each study site and estimated bankfull discharge by calibrating a 2-D flow model to minimize differences between modeled water-surface elevations and surveyed bankfull elevations. The estimates of bankfull discharge for study sites in Colorado range from 0.6 to 167 m^3/s.

[12] At gauged locations, the bankfull discharge can sometimes be identified graphically by a change in the stage-discharge relation (or area-width relation) [*Williams*, 1978]. We plotted stage-discharge relations for a dozen sites in Colorado and found that in all cases gauge height changes rather slowly with increasing discharge, and often, there is little visible change in the stage-discharge relation at bankfull flow (Figure 3). The asymptotic trends in gauge height in these streams are a reflection of both hydraulics and hydrology. Channel hydraulics govern the rate that gauge height (or depth) changes with discharge, and this commonly results in a curved stage-discharge relation. Snowmelt hydrology adds to this effect by limiting the intensity of runoff produced from a melting snowpack [*Cline*, 1997; *Pitlick*, 1994]. Both effects become important in our interpretation of the results presented later.

[13] We tested the general applicability of the daily flow models using similar measurements of flow and drainage basin characteristics in 32 unregulated streams and rivers in Idaho. The sites in Idaho are located in mountainous areas in the central portion of the state, with drainage areas ranging from 15 to 2694 km^2 (Table 2). These basins are mostly forested, although the density of forest cover decreases from north to south and with elevation. Bedrock lithologies are dominated by intrusive rocks of the Idaho batholith [*King et al.*, 2004; *Mueller et al.*, 2005] and headwater areas in most basins have been glaciated. Mean annual precipitation in the region varies from 30 to150 cm, with >60% of precipitation falling as snow [*Serreze et al.*, 1999]. Similar to Colorado, peak flows are generated primarily by spring snowmelt (Figure 2).

[14] For most of the study sites, we retrieved period-of-record mean daily discharge values from the U.S. Geological Survey National Water Information System (http://waterdata.usgs.gov/nwis). For several sites which are maintained by the U.S. Forest service (Table 2), we obtained daily flow values from the Boise Adjudication Team Web site (http://www.fs.fed.us/rm/boise/research/watershed/BAT/index.shtml), described by *King et al.* [2004]. We were not

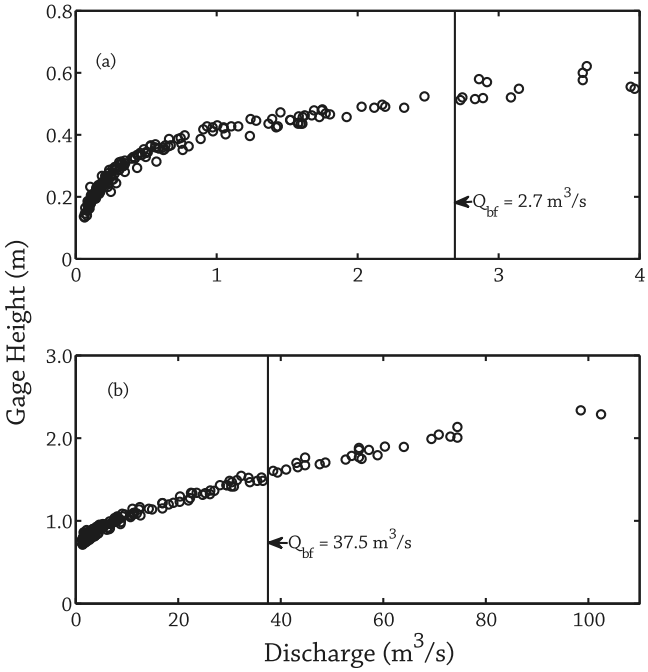

Figure 3. Stage-discharge relations for (a) Fraser River near Winter Park, Colo, USGS station 09022000, drainage area = 27.2 km^2, and (b) East River at Almont, Colo, USGS station 09112500, drainage area = 749 km^2.

involved in field data collection at the sites in Idaho; however, published descriptions of the field methods [*Castro and Jackson*, 2001; *King et al.*, 2004] indicate that bankfull discharges were estimated using techniques similar to those described above. Bankfull discharges of these streams and rivers vary from 2.5 to 326 m^3/s (Table 2).

2.3. Data Analysis

[15] Frequency distributions of daily flows ranging from the mean annual flow to the maximum observed discharge were constructed for each site by dividing the observations into 50 equal intervals of discharge, Q. The number of values, N_i, falling in each interval was counted, and those values were normalized by the bin width, dQ, to produce a frequency distribution where the number of observations is then independent of interval width [*Newman*, 2005]. In some cases, the number of days in a given discharge interval fell below 10; hence, two consecutive bins were joined. This only occurred for very high discharges and was done in order to ensure that the uncertainty in the number of values in each bin approximated a normal distribution [*Bevington and Robinson*, 2003; *Press et al.*, 2007; *Segura*, 2008]. The average frequency with which a flow is observed within a given interval of discharge, Q_i to Q_{i+1}, is thus

$$\int_{Q_i}^{Q_{i+1}} \frac{dN}{dQ} dQ, \tag{4}$$

where dN/dQ has the units of d yr^{-1}Q^{-1}.

[16] The parameters of the flow frequency distributions (EXP, LN, and BPL) were estimated by simultaneously varying individual combinations of the two parameters, over a uniform grid of more than 62,000 values and finding the parameter set that yielded the lowest overall χ^2 score [*Bevington and Robinson*, 2003; *Press et al.*, 2007]. χ^2 scores were calculated using a weighted sum of the squared differences between the observed and calculated frequencies of discharge,

$$\chi^2 = \sum_{i=1} \frac{[f_i - f(Q_i)]^2}{\sigma_i^2}, \tag{5}$$

where σ_i is the uncertainty associated with the observed frequencies, f_i. The χ^2 statistic is not used here to perform a rigorous goodness-of-fit test, since we are not attempting to fit the entire distribution of daily flows (only those above the mean), and we are not presuming that the observations forming the distributions are statistically independent. Daily flows are serially correlated; thus, there are inherent limitations in using standard goodness-of-fit tests to compare the observed frequency distributions to a set of hypothetical distributions. In this case, the distributions EXP, LN, and BPL are used only as mathematical functions for fitting the observations, and the χ^2 scores are not used as the basis for hypothesis testing. The parameter fits and resulting χ^2 scores simply provide a numerical value upon which we can index the overall performance of different models. To our knowledge there is no comparable parameter-fitting method or statistical test that gets around the problem of serial correlation in daily flows.

[17] Preliminary fits of the data using minimum χ^2 scores indicated that two out of the four parameters of the BPL distribution could be set to constant values. The average best fit values for the parameters α and β were 1.00 ± 0.03 and 6.98 ± 0.99; hence, these two parameters were set to 1 and 7, respectively. The decrease of χ^2 obtained by allowing all the four parameters to vary is small and does not justify the addition of two extra parameters with respect to the fit performed by holding α and β constant.

[18] The exponential, lognormal, and broken power law functions described above were fitted to the daily flow frequency distribution for each of the sites in Colorado. For a statistically acceptable fit, the value of the χ^2 needs to be close to the number of degrees of freedom in the fit [*Bevington and Robinson*, 2003; *Press et al.*, 2007]. When two or more different functions are compared, the one that provides the best description of the data is the one with the lowest χ^2.

3. Results

3.1. Selection of the Best Function to Describe Daily Flows

[19] The comparison of χ^2 minima on a site-by-site basis indicated that the BPL function provided the best fit in 27 out of 32 cases (Table 1). The exponential function provided a better fit in five cases but otherwise yielded relatively high χ^2 values (Table 1). The lognormal function produced the poorest fit, yielding χ^2 values up to five times the number of degrees of freedom. Given these results, it appears that the BPL provides a better fit to the distribution of snowmelt flows than either the exponential or lognormal functions.

[20] In order to evaluate the overall capability of the models to describe the whole data set, it is useful to introduce the concept of a reduced χ^2 (χ^2_ν), which is the value of

Table 2. Hydrologic Characteristics of the Selected Streams in Idaho, Length of Record Available, and Mean Basin Elevation, from *Berenbrock* [2002] and *Hortness* [2006][a]

USGS Gauge Number	Name	n (years)	DA (km^2)	Q_{bf} (m^3/s)	BE (m)	$d.f.$	χ^2	χ^2_ν	a_0	a_1	R(1y)
11111111[b]	Little Slate Creek	46	162.1	12.2[c]		27	32.6	1.2	80.7	11.4	0.85
11111112[b]	Lolo Creek	35	106.2	11.8[b]		30	24.6	0.8	72.4	11.8	0.78
11111113[b]	Main Fork Red River	36	128.7	9.4[c]		25	33.8	1.4	56.7	10.9	0.70
11111114[b]	Rapid River	88	279.7	17.7[c]		32	27.4	0.9	52.5	22.9	0.83
11111115[b]	South Fork Red River	35	98.9	7.3[c]		22	47.3	2.2	51.7	7.6	0.66
13120000	NF Big Lost River	62	297.1		2640	29	31.8	1.1	47.1	17.9	0.74
13120500	Big Lost River	58	1165.5		2618	34	28.9	0.8	44.3	58.4	0.75
13135500	Big Wood River	23	356.1	21.9[c]	2501	34	11.8	0.3	50.1	26.6	0.77
13185000	Boise River	96	2153.8	167[c]	1986	27	40.1	1.5	64.1	156.0	0.80
13186000	SF Boise River	61	1645.0	68.1[d]	2141	38	11.7	0.3	50.1	126.7	0.79
13196500	Bannock Creek	23	14.9		1619	22	78.3	3.6	50.1	0.3	0.64
13200000	Mores Creek	56	1033.0	26.4[d]	1546	25	24.7	1.0	59.3	43.1	0.69
13200500	Robie Creek	21	40.9		1426	17	81.7	4.8	44.3	1.5	0.59
13235000	South Fork Payette River	66	1181.0	86.4[c]	2080	33	22.1	0.7	63.1	109.4	0.83
13240000	Lake Fork Payette River	61	126.1	11.2[d]	2118	34	25.5	0.7	41.1	29.3	0.77
13251500	Weiser River	63	94.5		1402	24	14.4	0.6	21.2	10.3	0.67
13258500	Weiser River	67	1567.0	37.6[d]	1417	14	154.4	11.0	79.4	67.4	0.68
13261000	Little Weiser River	36	205.0		1619	30	10.8	0.4	65.1	15.3	0.77
13295000	Valley Creek	66	380.7	24.1[c]	2231	32	24.6	0.8	59.3	26.0	0.84
13295500	Salmon River	35	1297.6		2373	36	14.0	0.4	64.1	78.2	0.84
13296000	Yankee River	27	505.1		2436	33	36.6	1.1	39.8	36.6	0.71
13296500	Salmon River	72	2077.2	118[c]	2375	34	25.5	0.8	54.1	137.2	0.81
13297330	Thompson Creek	35	75.4	2.5[c]	2322	25	43.1	1.7	43.0	2.9	0.66
13297355	Squaw Creek	35	185.4	5.1[c]	2356	27	49.7	1.8	36.3	6.8	0.68
13298000	Salmon River	19	1377.9		2467	21	36.6	1.7	48.6	35.1	0.66
13308500	MF Salmon River	43	346.5		2281	35	12.0	0.3	42.3	45.0	0.80
13309220	Middle Fork Salmon River	16	2693.6	214[c]	2192	19	6.4	0.3	47.1	214.0	0.71
13310500	SF Salmon River	32	238.3		2021	35	29.5	0.8	42.3	26.5	0.82
13310700	SF Salmon River	35	855.0	70.8[c]	1945	32	15.9	0.5	50.9	86.8	0.76
13311000	EF South Frk Salmon River	28	51.0	9.6[d]	2354	29	27.8	1.0	40.4	4.4	0.73
13313000	Johnson Creek	79	552.0	39.7[c]	2175	33	22.4	0.7	37.4	73.9	0.78
13337500	SF Clearwater River	30	676.0		1570	29	12.7	0.4	50.9	46.1	0.77

[a] n, length of record available; BE, Mean Basin Elevation; $d.f.$, degrees of freedom; χ^2, reduced χ^2 (χ^2_ν), and parameters, a_0 and a_1, of the fit of the broken power law functions to the daily flow distribution, and annual autocorrelation (R(1y)) of daily flows.
[b] Flow data obtained from *King et al.* [2004]. The gauge number is arbitrary.
[c] Reference for Q_{bf}: *King et al.* [2004].
[d] Reference for Q_{bf}: *Castro and Jackson* [2001].

the χ^2 divided by the number of degrees of freedom. The average value of χ^2_ν gives an estimate of how well a particular function describes the complete data set. An excellent fit should yield $\chi^2_\nu \leq 1$. The BPL function provides the best score with $<\chi^2_\nu> = 0.95$, followed by the EXP with $<\chi^2_\nu> = 1.40$ and by the LN with $<\chi^2_\nu> = 2.26$ (Table 1). This result corroborates the choice of the BPL model as the functional form to describe the frequency distribution of intermediate to high daily flows in snowmelt dominated streams.

3.2. Development of a Regional Model for Colorado

[21] Figure 4 presents the fit of the BPL function to the frequency distribution of daily flows at six representative sites in Colorado. The χ^2_ν of the fit on these six basins varies between 0.48 and 1.12, which represents the range observed for most of the data (Table 1). The best-fit values of a_0 and a_1 for all 32 sites are plotted versus drainage area (DA), bankfull discharge (Q_{bf}), and mean basin elevation (BE) in Figure 5. Linear regression was used to find the best relationship between the parameters a_0 and a_1 and drainage basin characteristics. The results of this analysis indicated that neither a_0 nor a_1 was strongly correlated with BE (Table 3). Therefore, elevation was discarded as a scaling parameter. Both a_0 and a_1 were positively correlated with DA and Q_{bf} (Figure 5). The statistics of these regressions indicate that Q_{bf} and DA have very similar predicting power for a_0 and a_1 (Table 3), which is not surprising considering that DA and Q_{bf} are strongly correlated (Figure 6). DA is best for describing both a_0 and a_1 (Table 3). Therefore, DA was chosen to formulate the regional model. DA is a robust descriptor of the amount of runoff occurring in a given area, and this parameter has also been observed by many others as the best scaling parameter to transfer similarity properties of hydrologic processes [e.g., *Gupta et al.*, 1994; *Vogel and Sankarasubramanian*, 2000; *Ogden and Dawdy*, 2003; *Furey and Gupta*, 2005].

[22] The regional model is described by the following equation:

$$\frac{dN}{dQ} = \frac{a_0/a_1}{(Q/a_1) + (Q/a_1)^7}, \tag{6}$$

with the parameters a_0 and a_1 scaling as a function of the drainage area, DA:

$$a_0 = (31.04 \pm 2.7)\,\mathrm{DA}^{0.061\pm0.019} \text{ and} \tag{7}$$

$$a_1 = (0.213 \pm 0.027)\,\mathrm{DA}^{0.835\pm0.028}. \tag{8}$$

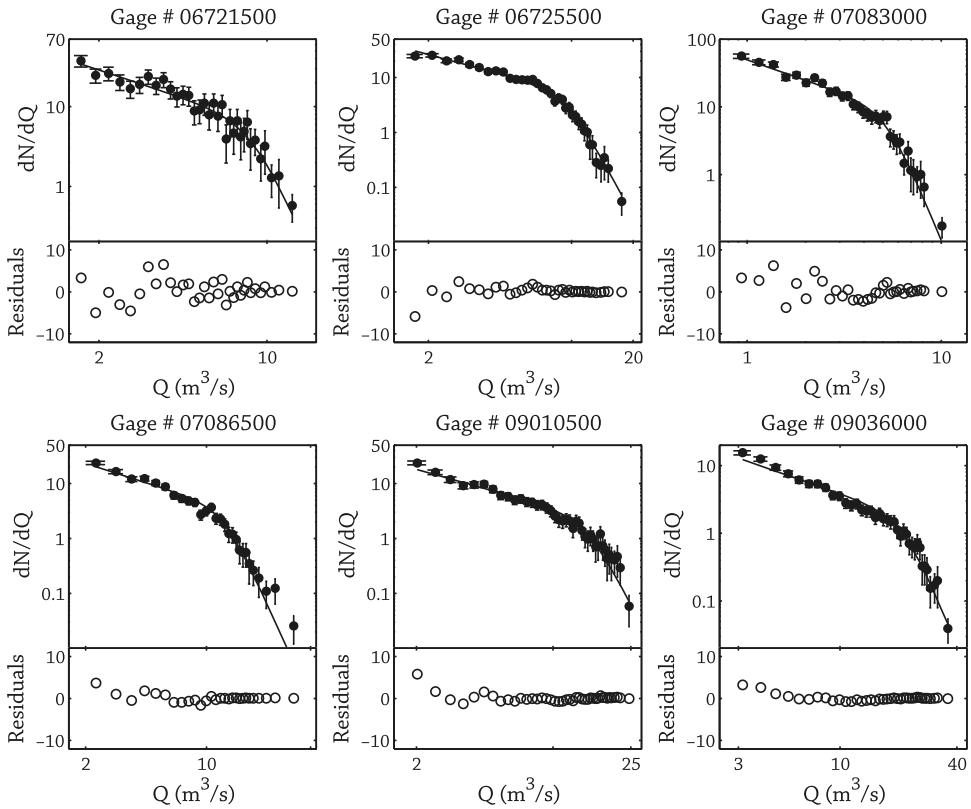

Figure 4. Fits of the broken power law (BPL) function to the daily flow frequency distributions of 6 sites in Colorado. The units of the y-axis are the same as in Figure 1b.

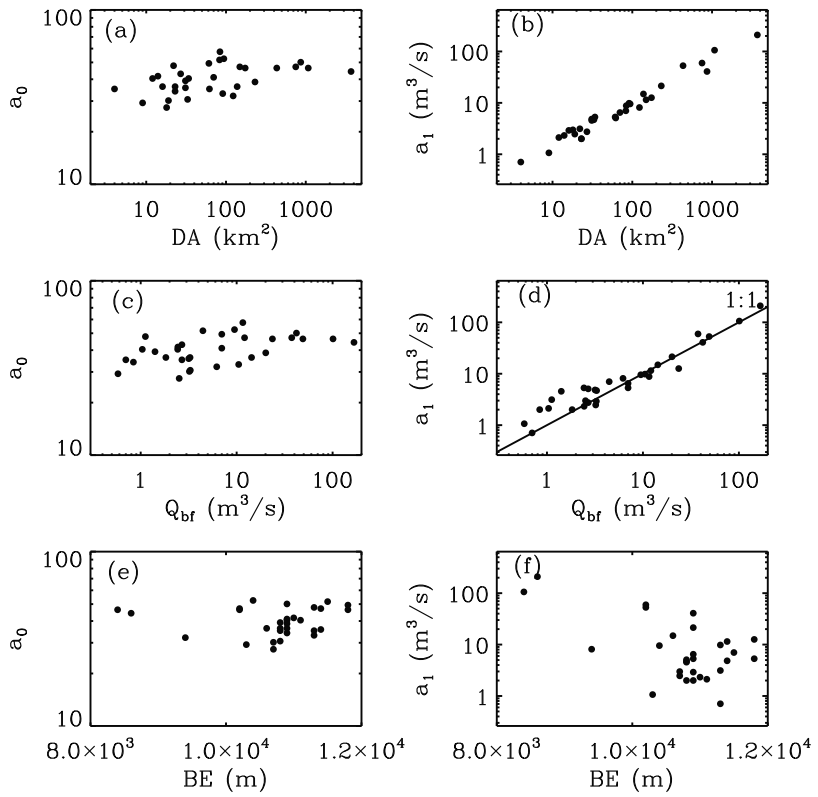

Figure 5. Parameters a_0 and a_1 of the broken power law (BPL) function versus drainage area (DA), bankfull discharge (Q_{bf}), and mean basin elevation (BE) for 32 sites in Colorado.

Table 3. Summary and Statistics for Regression Between the Parameters, a_0 and a_1, of the Broken Power Law and Drainage Area, Bankfull Flow, and Mean Basin Elevation for 32 Basins in Colorado[a]

Y	X	*a*	*b*	r^2	*P*
a_0	DA	31.0 (2.7)	0.061 (0.019)	0.243	0.0041
a_0	Q_{bf}	35.8 (1.7)	0.064 (0.021)	0.240	0.0044
a_0	BE	28.9 (118.7)	0.0335 (0.442)	<0.001	0.94
a_1	DA	0.213 (0.027)	0.835 (0.028)	0.966	≪0.0001
a_1	Q_{bf}	1.55 (0.16)	0.867 (0.046)	0.922	≪0.0001
a_1	BE	[2.0 (48.2)]1E41	–10 (2.6)	0.341	0.0007
a_1/DA	DA	0.213 (0.027)	–0.165 (0.028)	0.530	≪0.0001

[a](Figure 5): *a* and *b* are parameters of the power law relation, $Y = aX^b$; values shown in parenthesis are standard errors of the regression coefficients, SE_a and SE_b; r^2 is the coefficient of determination; and *P* is the significance probability.

[23] Using these relations, the number of days per year that a discharge within a particular range is observed can be computed as

$$\text{number of days} = \frac{a_0}{a_1}\int_{Q_i}^{Q_{i+1}} \frac{1}{(Q/a_1)+(Q/a_1)^7}\,dQ, \qquad (9)$$

where a_0 and a_1 are given by equations (7) and (8).

[24] The exponent in the relation between a_1 and DA is less than one, indicating that the location of the inflection point in the distribution of daily flows does not change in direct proportion to DA. In order to investigate the scaling properties of a_1 with DA, the values of a_1 were normalized by DA and plotted versus DA (Figure 7). If the location of the inflection point between intermediate and high flows varied in proportion to drainage area, this figure would depict no correlation. Instead, Figure 7 indicates that there is an inverse correlation between a_1/DA and DA ($r^2 = 0.53$; $P \ll 0.0001$) (Table 3). This result implies that as drainage area increases the location of the inflection point, a_1, occurs at consistently lower values of a_1/DA. In other words, it appears that as DA increases, the frequency of high-flow events consistently decreases downstream. We examined the relation between a_1/DA and DA for subsets of gauges within two individual drainage basins (Arkansas River and Williams Fork) and found that there was no difference in the trends within the individual basins and the trend defined for the region as a whole.

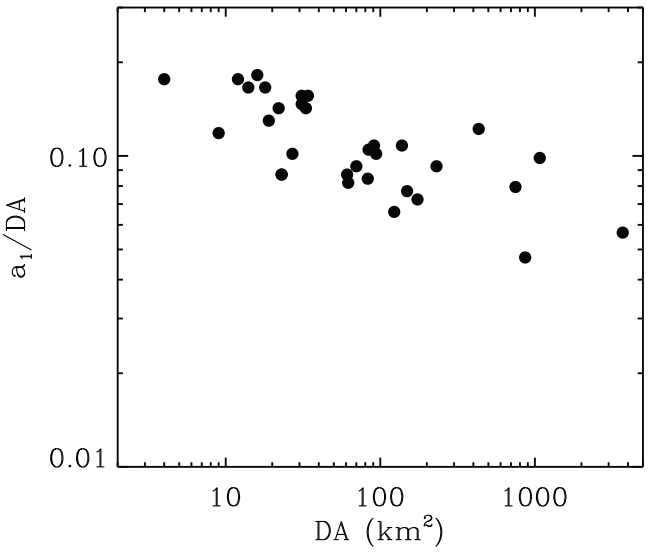

Figure 7. Relation between the parameter a_1 of the broken power law function (BPL) normalized by drainage area (DA) and DA for 32 sites in Colorado.

[25] The relationships shown in Figures 5–7 indicate that both the location of the inflection point in the BPL (a_1) and the magnitude of Q_{bf} grow less than linearly with DA. Furthermore, the cluster of points around the 1:1 line in Figure 5d indicates that the values of Q_{bf} and a_1 are very closely related, especially for sites with Q_{bf} above 10 m^3/s and drainage areas above 120 km^2. The break in the frequency distribution implies that there is a shift in the relation between flow frequency and discharge at almost precisely the point where flows reach bankfull. The observed relation between a_1 and Q_{bf} suggests that in snowmelt-dominated streams the probability associated with overbank flows drops off very quickly, whereas the discharges that are important for shaping the channel (flows higher than about 67% of Q_{bf}) [*Mueller et al.*, 2005] occur almost every year.

[26] Since the flow records from the 32 sites do not encompass the same time period and they include observations in some cases going back to the early 1900s, an additional analysis was performed to ensure that the results presented above were not an expression of secular climatic variability. The same analysis was performed for a subsample of the Colorado data set that includes 23 gauges with overlapping daily flow records of 28 years between 1966 and 1994. Statistically indistinguishable results were found. This indicates that the behavior of the distribution parameters a_0 and a_1 is not governed by short-term variations in hydrology [*Segura*, 2008].

[27] The regional model described by equation (6) together with the relation between DA and Q_{bf} (Figure 6) were used to compare downstream changes in the frequency of flows between $0.2Q_{bf}$ and Q_{bf} and flows above Q_{bf} for a hypothetical high-elevation stream draining an area of 4000 km^2.

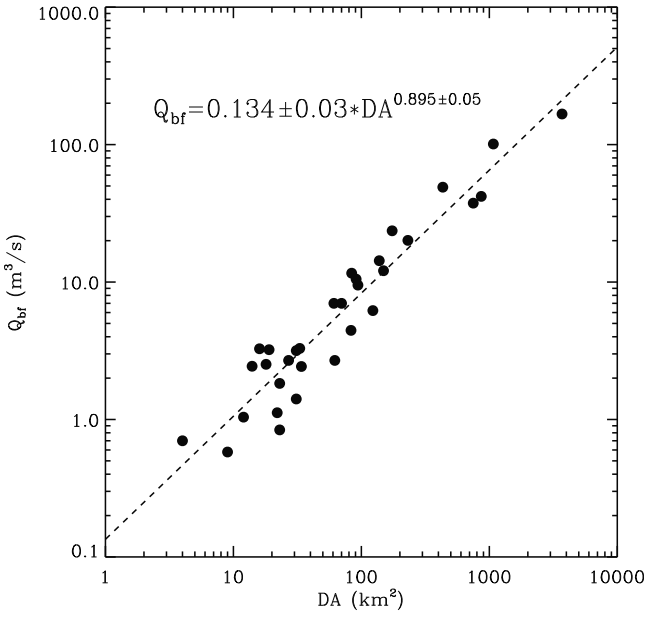

Figure 6. Relation between bankfull discharge (Q_{bf}) and drainage area (DA) for 32 sites in Colorado.

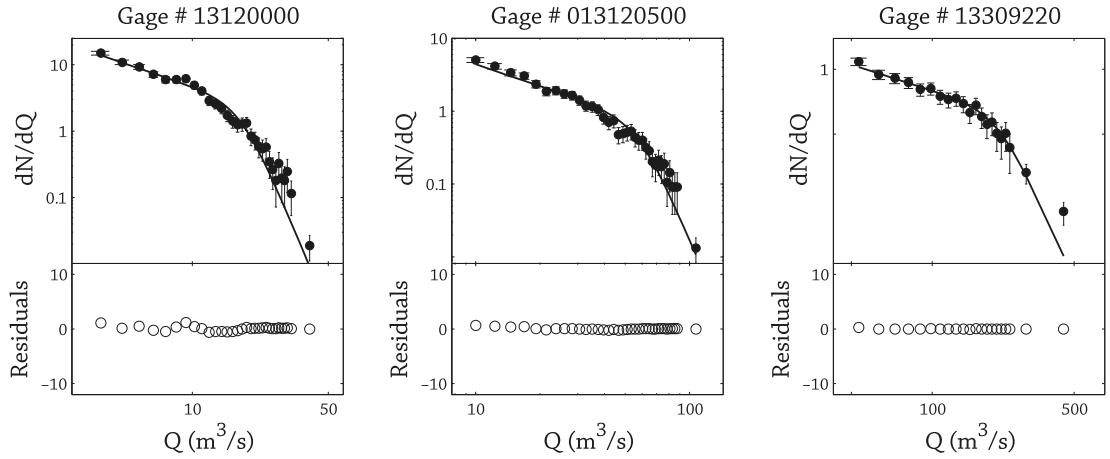

Figure 8. Fits of the broken power law (BPL) function to daily flows for three representative sites in Idaho. The units of the y-axis are the same as in Figure 1b.

The results indicate that the frequency of flows between $0.2Q_{bf}$ and Q_{bf} increases downstream from 64 d/yr in the headwaters to 81 d/yr at the mouth. In contrast, the frequency of overbank flows, $Q > Q_{bf}$, decreases downstream from 15 d/yr in the headwaters to 6 d/yr near the mouth. The downstream difference in frequency arises because the exponent in the relation between a_1 and DA (equation (8)) is less than one. Thus, even within a region of relatively homogeneous climate and land cover, the frequency of bankfull discharge appears to decrease downstream.

[28] The observation that basins with small drainage area experience more frequent high flows, but less frequent intermediate flows than sites with large drainage areas suggests that daily flow frequency distributions of snowmelt-dominated streams in Colorado exhibit multiscaling properties. Streams draining small basins are characterized by flow frequency distributions with larger standard deviations (larger tails in both extremes) compared to rivers draining large basins.

3.3. Application of the Model to Basins in Idaho

[29] We tested the general applicability of the broken power law using data from similar-sized basins in central Idaho. Figure 8 presents the BPL fit to the frequency distributions of daily flows from three representative gauging stations in this region. From Figure 8, it is apparent that the BPL function fits the distributions of daily flows at these sites relatively well. The χ^2_ν values computed from the parameter fits of the BPL to the sites in Idaho (Table 2) are comparable to the sites in Colorado and in only a few cases is the χ^2_ν much greater than 1.0, the average for Colorado.

[30] Differences in the seasonality and intensity of runoff (snowmelt versus rainfall) evidently determine how well the BPL function fits the distribution of intermediate to high flows. We investigated these hydroclimatic effects further by evaluating the annual correlation of daily flows in the Colorado and Idaho study regions. Figure 9 shows a series of annual hydrographs and corresponding 1 year autocorrelation functions for representative gauging stations in

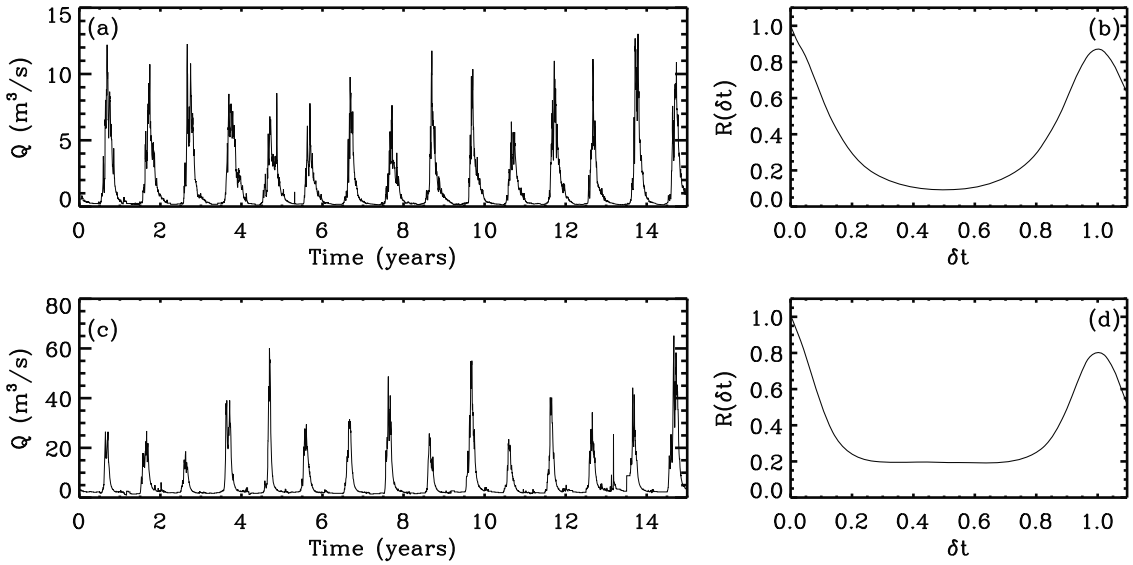

Figure 9. Fifteen year hydrograph and autocorrelation of daily flows of (a and b) North St. Vrain River, Colo, USGS station 06721500 and (c and d) MF Salmon River, Idaho, USGS station 13308500.

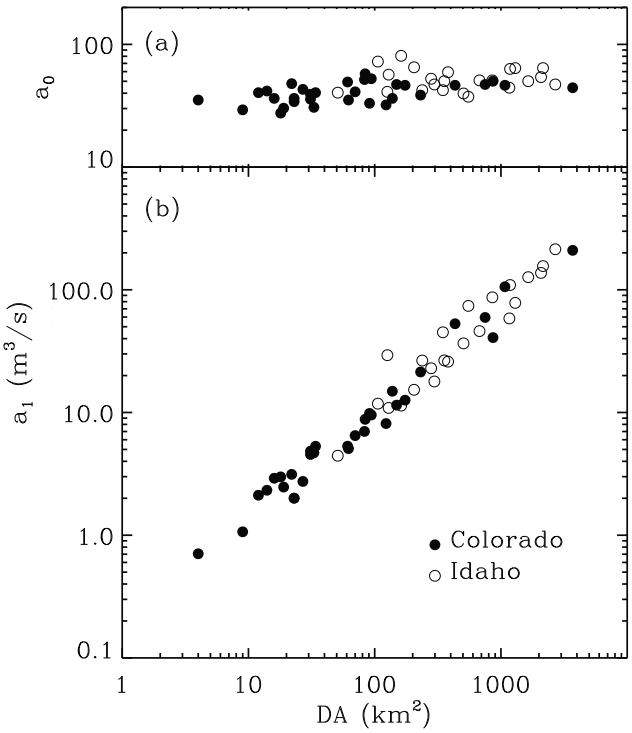

Figure 10. Parameters a_0 and a_1 of the broken power law (BPL) function versus drainage area (DA) for sites in Colorado and Idaho with 1 year autocorrelation greater than 0.70.

these two regions. The 1 year autocorrelation, $R(1y)$, is computed as

$$R(\delta t) = \frac{\int Q(t)Q(t+\delta t)\mathrm{d}t}{\int Q^2(t)\mathrm{d}t}, \qquad (10)$$

where δt is the time shift (in this case 1 year), and $Q(t)$ is the discharge on a given day. In the examples shown in Figure 9, the autocorrelation functions exhibit a distinct peak at $\delta t = 1$. We repeated these calculations for all of the gauging stations listed in Tables 1 and 2 and found that the 1 year autocorrelation, $R(1y)$, exceeded 0.70 at all of the sites in Colorado and 72% of the sites in Idaho (Tables 1 and 2). A value of $R(1y) \sim 0.70$ might thus be used as a criterion for distinguishing between strong/weak correlations in flow and for determining in advance whether the BPL might be more applicable for fitting daily flow frequency distributions than other candidate functions.

[31] Figure 10 shows relations between the best-fit parameters of the BPL, a_0 and a_1, and drainage area, DA, for the 55 sites in Idaho and Colorado where $R(1y) > 0.70$. The same scale is used for both a_0 and a_1 to illustrate the much greater range in a_1 compared to a_0. The parameter values from each region broadly overlap, with the slightly higher values in Idaho reflecting larger drainage areas. We computed separate regression equations for each data set and performed an analysis of covariance (ANCOVA) to compare the slopes and intercepts of the separate relations. The ANCOVA results indicate that the slopes and intercepts of the separate relations are not significantly different ($P \gg 0.05$); hence, we combined the data to form single relations for a_0 and a_1. Significance tests of the regression equations (Table 4) indicate that the best-fit relations for a_0 and a_1 are statistically significant at the $P < 0.001$ level.

[32] In section 3.2 we presented a relation between a_1/DA and DA showing that the inflection point between intermediate and high flows does not scale in proportion to DA. Adding the Idaho data to that relation (Figure 11) reinforces this point and supports the conclusion made earlier that the inflection point in the frequency distribution of snowmelt flows shifts as drainage area increases. Significance tests of the regression parameters again indicate there is no significant difference in the slopes and intercepts of the separate relations ($P > 0.40$), and the relation between a_1/DA and DA is statistically significant (Table 4). Figure 11b shows that the close association between bankfull discharge, Q_{bf}, and a_1 is also maintained across the two data sets. The results in Figure 11 thus suggest that the scale-dependent changes in the frequency of intermediate to high flows, and the bankfull flow, in particular, appears to be a characteristic of these snowmelt-dominated systems.

4. Interpretation

[33] The river systems considered in this analysis represent a specific class of channels draining rugged, high-elevation areas where runoff is generated principally by snowmelt. Sediment supply to these channels is not especially high; however, the sites are all located in alluvial reaches that are relatively free of flow regulation; thus, we assume that the observed channel characteristics have evolved over time in response to the prevailing water and sediment supply. We have not assumed, however, that these processes act with the same intensity within a basin and have presented results indicating that the frequency of bankfull discharge varies with scale. In the sections that follow, we consider processes that might lead to scale-dependent changes in the frequency of bankfull flow.

4.1. Attenuation and Storage

[34] Peak discharges generally attenuate as they move through the channel network, and it has been suggested in several studies that storage within the channel and adjacent floodplain can alter the magnitude and frequency distribution of peak flows downstream [*Wolff and Burges*, 1994; *Woltemade and Potter*, 1994; *Gupta and Dawdy*, 1995]. In a more recent study, *Dodov and Foufoula-Georgiou* [2005] found that, in contrast to our results, the frequency of

Table 4. Summary and Statistics for Regression Between the Parameters, a_0 and a_1, of the Broken Power Law and Drainage Area for Basins in Colorado and Idaho[a]

Y	No.	a	b	r^2	P
a_0	64	30.2 (2.7)	0.078 (0.017)	0.261	<0.0001
a_1	64	0.164 (0.029)	0.871 (0.033)	0.917	≪0.0001
a_0[b]	55	30.6 (2.6)	0.075 (0.016)	0.289	≪0.0001
a_1[b]	55	0.197 (0.023)	0.858 (0.022)	0.966	≪0.0001
a_1/DA	64	0.164 (0.029)	–0.129 (0.033)	0.196	0.0002
a_1/DA[b]	55	0.197 (0.023)	–0.142 (0.022)	0.437	≪0.0001

[a](Figures 10 and 11): No. is the number of basins considered, and a and b are parameters of the power law relation, $Y = aX^b$; values shown in parenthesis are standard errors of the regression coefficients, SE_a and SE_b; r^2 is the coefficient of determination; and P is the significance probability.
[b]Regression based on the data of Colorado and Idaho combined excluding sites with 1 year autocorrelation less than 70%.

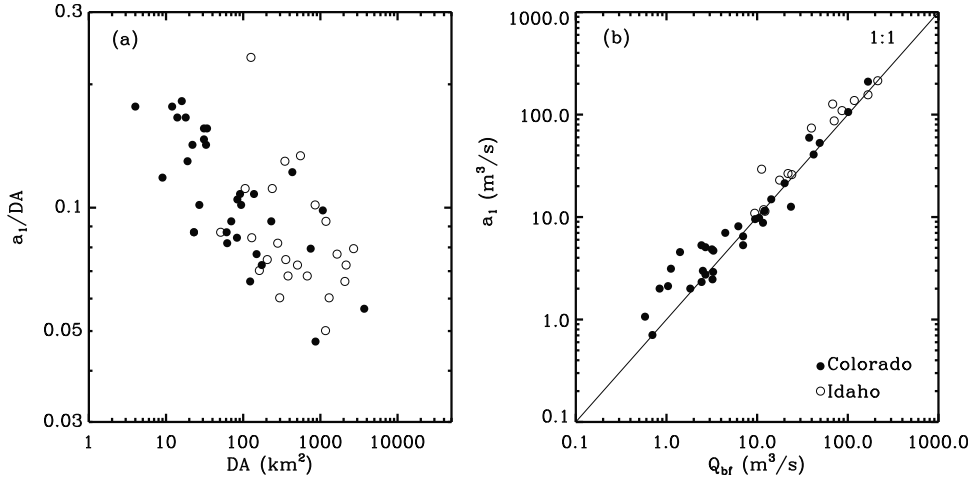

Figure 11. (a) Relation between the parameter a_1 of the broken power law function, normalized by drainage area (DA), and DA; (b) relationship between a_1 and Q_{bf} across basins in Colorado and Idaho excluding sites with 1 year autocorrelation less than 0.70.

flows exceeding Q_{bf} increased downstream. These authors suggested that as slope decreases and channels become more sinuous downstream, the added resistance to flow over point bars and vegetated banks decreases the celerity of flood waves, thus, generating higher stages for longer periods of time.

[35] We evaluated the potential influence of attenuation and storage on flow frequency by comparing continuous records of discharge at two gauges in the Williams Fork basin in Colorado. The two main tributaries of the Williams Fork are gauged just above the point where they join, and the main stem is gauged another 5 km downstream where the river meanders through a valley with a wide floodplain. We hypothesized that if changes in slope and sinuosity affect the translation of peak flows, we should see clear differences in the hydrographs at upstream and downstream gauges. We selected 1995, a year of high runoff, and compared simultaneous 15 min records of discharge at the upstream and downstream gauges, normalizing each value of discharge by drainage area to account for differences in scale. Figure 12 shows continuous records for 1995, in which there were two peaks, and the bankfull discharge was exceeded frequently at both gauges. It appears that in the period leading up to the first peak (days 30–40, Figure 12b) unit discharges at the two gauges tracked each other closely. If there was much attenuation in the reach between the gauges, it was probably offset by inputs from tributaries. During the peak (days 45-55, Figure 12b), unit discharges at the downstream gauge were generally lower than the upstream gauge, suggesting there was some storage associated with the transition to overbank flow. The hydrograph for the second peak (Figure 12c) exhibits a different pattern, with little difference in discharge during the peak, but higher discharges at the downstream gauge on the falling limb. The crossover in upstream-downstream discharge relations is consistent with the hypothesis that the floodplain will act first as a sink, then as a source for downstream reaches, however, the differences here are probably too small to conclude that floodplain storage has much influence on the frequency of bankfull flow.

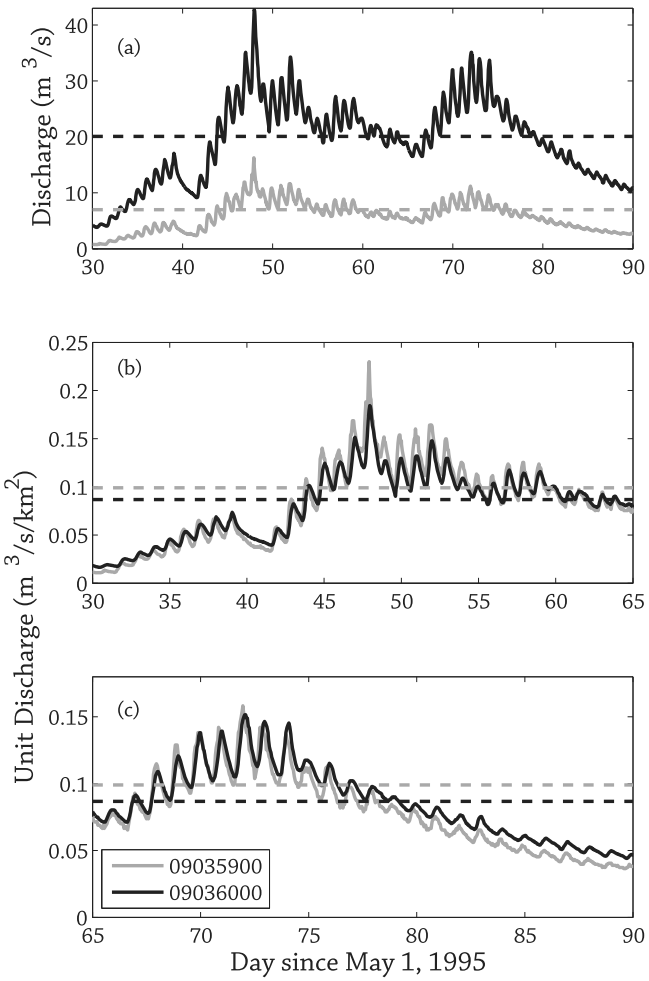

Figure 12. Records of instantaneous discharge, May–July 1995, for two gauges in the Williams Fork watershed. Gauge 09035900 drains 70.3 km^2 and is located on a tributary with limited floodplain area. Gauge 09036000 drains 231 km^2 and is located in a wide valley with an extensive floodplain area. Dashed lines indicate bankfull discharge.

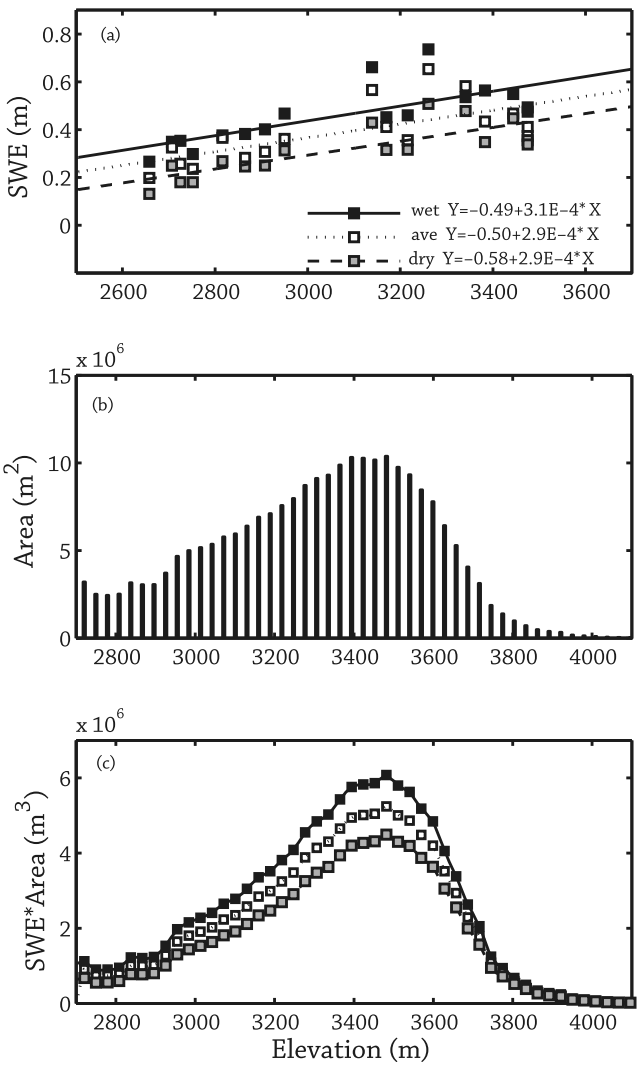

Figure 13. (a) Relationship between snow water equivalent (SWE) and elevation for 19 stations in the upper Colorado River region during wet, average, and dry conditions; (b) frequency distribution of elevation in the Williams Fork basin (drainage area = 231 km^2) derived from a 10 m digital elevation model; and (c) volumetric water content for wet, average, and dry years.

4.2. Spatial Variability in Runoff

[36] We explored another possibility that the differences in bankfull flow frequency are related to spatial variations in the volume of runoff produced by snowmelt. Data from snow telemetry (SNOTEL) stations in the upper Colorado River basin indicate that the April 1 snow water equivalent (SWE) increases linearly with elevation (Figure 13a). However, the terrain over which snow is distributed is very irregular; thus, the spatially averaged water content becomes a more complex function of basin hypsometry (area above a given elevation). Figure 13b shows the relation between area and elevation in the drainage basin of the Williams Fork, derived from a digital elevation model. This distribution exhibits a pattern typical of high-relief terrain where the relation between area and elevation increases more or less continuously to a point (~3500 m) then drops off sharply. If we combine the relations for SWE in Figure 13a with the distribution of area in Figure 13b, we get relations for volumetric water content in wet, average, and dry years, as shown in Figure 13c. These results suggest that in alpine-subalpine basins in Colorado, the majority of runoff is derived from areas that lie between about 3100 and 3700 m in elevation. At elevations higher and lower than this, the volume of water held in the snowpack decreases, and differences between wet and dry years diminishes. These results suggest that in small headwater basins the volume of runoff produced in any given year is never much higher or lower than the average. Consequently, the geomorphic processes which determine the bankfull hydraulic geometry act with more or less the same intensity each year, leading to a higher frequency of bankfull flows. As drainage area increases, the amount of runoff generated per unit area decreases, and the differences between wet and dry years become more pronounced. In addition, at elevations between about 3000 and 2500 m, streams pass beyond the glacial limit and into more sparsely vegetated areas where the sediment supply increases. Results from our previous studies of these river systems [*Mueller and Pitlick*, 2005; *Pitlick et al.*, 2008; *Segura*, 2008] indicate that, as drainage area and sediment supply increase, channel and bed material properties evolve downstream to produce a bed that is less armored and thus able to sustain low to moderate levels of bed load transport over a wider range of discharges. We suggest, therefore, that the upstream-downstream transitions in flow frequency in these river systems reflect not only the spatial variations in runoff but also the way in which the channel geometry and bed material evolve downstream to convey higher sediment loads with proportionally less water.

5. Conclusions

[37] The goal of this paper was to develop a regional flow frequency model that could then be used to examine the scaling behavior of channel-forming discharges. The results indicate that the frequency distribution of daily flows in snowmelt-dominated river systems can be reproduced relatively well with a two-parameter broken power law distribution (BPL). The BPL model appears to be most applicable to stream systems with predictable patterns of runoff, i.e., daily flows with 1 year autocorrelation above 0.7. The two parameters of the BPL are both strongly correlated with drainage area, and based on these correlations, a regional model capable of predicting the frequency distribution of intermediate to high flows was formulated. According to the derived model, the parameter which defines the inflection point in the BPL distribution, a_1, increases with drainage area, DA; however, we find that the relation between a_1 and DA is nonlinear. The shift in the inflection point apparently reflects systemwide changes in hydrology which lead to a downstream decrease in the frequency of high flows (and an increase in the frequency of intermediate flows). The relation between a_1 and DA thus suggests that daily flows in snowmelt-dominated stream systems exhibit multiscaling behavior. We also find that a_1 is strongly and positively correlated to the bankfull discharge, Q_{bf}. When coupled with the relation between a_1 and DA, this last result indicates that there is a scale-dependent change in the frequency of channel-forming flows.

[38] Our analysis of the timing and translation of diurnal variations in flow in the Williams Fork basin (DA = 231 km^2) suggests that the volumes of water that go into floodplain storage during the height of snowmelt runoff are relatively small in comparison to discharges conveyed within the channel. It appears that, in these types of river systems, there is an upper limit to the intensity of runoff produced by snowmelt; hence, attenuation due to within-channel or overbank storage does not strongly influence the distribution of daily flows. These effects would likely be more pronounced in hydroclimatic regions where floods are produced by rainfall (or rain on snow) and where floodplains are inundated to greater depths. We suggest that a better case can be made for the influence of snow cover and topography, which combine to generate a peak in snowmelt runoff at intermediate drainage areas. Our hypothesis warrants further testing, but we infer from the analysis of snow cover and topography, plus results from previous work on these same river systems, that channels evolve downstream to produce widths, depths, and slopes that can sustain low to moderate levels of bed load transport over a wider range of discharges.

[39] **Acknowledgments.** The research reported here was funded in part by grants from the National Science Foundation (BCS-9986338) and the U.S. Forest Service (03-CS-11221625-122). Peter Furey, Richard Vogel, Kyungrock Paik, and Sankar Arumugam provided thoughtful comments on our analysis and interpretation of the results. We thank Andy Bock for his help in generating the area-elevation relations for the Williams Fork Basin and several other watersheds in Colorado. We would also like to thank Martin Doyle, Ellen Wohl, and two anonymous reviewers for their thorough reviews of an early version of this manuscript; the journal editor, Tom Torgerson, and associate editor Fred Ogden also provided helpful suggestions.

References

Aban, I. B., M. M. Meerschaert, and A. K. Panorska (2006), Parameter estimation for the truncated Pareto distribution, *J. Am. Stat. Assoc.*, *101*, 270–277.

Andrews, E. D. (1984), Bed-material entrainment and hydraulic geometry of gravel bed rivers in Colorado, *Geol. Soc. Am. Bull.*, *95*, 371–378.

Andrews, E. D. (1994), Marginal bed load transport in a gravel bed stream, Sagehen Creek, California, *Water Resour. Res.*, *30*, 2241–2250.

Archfield, S. A., R. M. Vogel, and S. L. Brandt (2007), Estimation of flow duration curves at ungaged sites in southern New England, in *Proceedings, ASCE World Environmental and Water Resources Congress 2007*, doi 10.1061/40927(243)407, pp. 1–14.

Berenbrock, C. (2002), Estimating the magnitude of peak flows at selected recurrence intervals for streams in Idaho, *U.S. Geol. Surv. Water Resources Investigation Rep. 2002-4170*.

Bevington, P. R., and D. K. Robinson (2003), *Data Reduction and Error Analysis for The Physical Sciences*, McGraw-Hill, New York.

Burroughs, S. M., and S. F. Tebbens (2001), Upper truncated power laws in natural systems, *Pure Appl. Geophys.*, *158*, 741–757.

Castellarin, A., G. Galeati, L. Brandimarte, A. Montanari, and A. Brath (2004), Regional flow-duration curves: reliability for ungaged basins, *Adv. Water Resour.*, *27*, 953–965.

Castro, J. M., and P. L. Jackson (2001), Bankfull discharge recurrence intervals and regional hydraulic geometry relationships: Patterns in the Pacific Northwest, USA, *J. Am. Water Res. Assoc.*, *37*(5), 1249–1262.

Chaplin, J. J. (2005), Development of regional curves relating bankfull-channel geometry and discharge to drainage area for streams in Pennsylvania and selected areas of Maryland, *U.S. Geol. Surv. Scientific Investigations Rep. 2005–5147*.

Cline, D. W. (1997), Effect of seasonality of snow accumulation and melt on snow surface energy exchanges at a continental alpine site, *J. Appl. Meteorol.*, *36*, 32–51.

DeRose, R. C., M. J. Stewardson, and C. Harman (2008), Downstream hydraulic geometry of rivers in Victoria, Australia, *Geomorphology*, *99*, 302–316, doi:10.1016/j.geomorph.2007.11.008.

Dodov, B., and E. Foufoula-Georgiou (2005), Fluvial processes and streamflow variability: Interplay in the scale-frequency continuum and implications for scaling, *Water Resour. Res.*, *41*, W05005, doi:10.1029/2004WR003408.

Doyle, M. W., E. H. Stanley, D. L. Strayer, R. B. Jacobson, and J. C. Schmidt (2005), Effective discharge analysis of ecological processes in streams, *Water Resour. Res.*, *41*, W11411, doi:10.1029/2005WR004222.

Doyle, M. W., and C. A. Shields (2008), An alternative measure of discharge effectiveness, *Earth Surf. Processes Landforms*, *33*, 308–316.

Dunne, T., and L. B. Leopold (1978), *Water in Environmental Planning*, 818 pp., W. H. Freeman, New York.

Emmett, W. W. (1975), The channels and waters of the Upper Salmon River area, Idaho, *U.S. Geol. Surv. Prof. Pap., 870-A*.

Fennessey, N., and R. M. Vogel (1990), Regional flow-duration curves for ungaged sites in Massachusetts, *J. Water Resour. Plann. Manage.*, *116*, 530–549.

Furey, P. R., and V. K. Gupta (2005), Effects of excess rainfall on the temporal variability of observed peak-discharge power laws, *Adv. Water Resour.*, *28*, 1240–1125.

Goodwin, P. (2004), Analytical solutions for estimating effective discharge, *J. Hydraul. Eng.*, *130*, 729–738.

Gupta, V. K., and D. R. Dawdy (1995), Physical interpretations of regional variations in the scaling exponents of flood quantiles, *Hydrol. Processes*, *9*, 347–361.

Gupta, V. K., O. J. Mesa, and D. Dawdy (1994), Multiscaling theory of flood peaks: Regional quantile analysis, *Water Resour. Res.*, *30*, 3405–3421.

Hortness, J. E. (2006), Estimating low-flow frequency statistics for unregulated streams in Idaho, *U.S. Geol. Surv. Scientific Investigations Rep. 2006–5035*.

Jarrett, R. D. (1990). Paleohydrologic techniques used to define the spatial occurrence of floods. *Geomorphology*, *3*, 181–195.

Jarrett, R. D., and J. E. Costa (1988), Evaluation of the flood hydrology in the Colorado Front Range using precipitation, streamflow, and paleoflood data, *U.S. Geol. Surv. Water Resources Investigations Rep. 87–4117*.

Keaton, J. N., T. Messinger, and E. J. Doheny (2005), Development and analysis of regional curves for streams in the non-urban Valley and Ridge Physiographic Province, Maryland, Virginia, and West Virginia, *U.S. Geol. Surv. Scientific Investigations Rep. 2005–5147*.

King, J. G., W. W. Emmett, P. J. Whiting, R. P. Kenworthy, and J. J. Barry (2004), Sediment transport data and related information for selected coarse-bed streams and rivers in Idaho, *Gen. Tech. Rep. RMRS-GTR-131*, 26 pp., Rocky Mt Res. Stn., U.S. Dep of Agric. For. Serv., Fort Collins, Colo. (Available at http://www.fs.fed.us/rm/boise/research/watershed/BAT/index.shtml).

Knighton, A. D. (1998), *Fluvial Forms and Processes—A New Perspective*, 383 pp., Edward Arnold, London.

Mueller, E. R., and J. Pitlick (2005), Morphologically based model of bed load transport capacity in a headwater stream, *J. Geophys. Res.*, *110*, F02016, doi:10.1029/2003JF000117.

Mueller, E. R., J. Pitlick, and J. Nelson (2005), Variation in the reference Shields stress for bed load transport in gravel bed streams and rivers, *Water Resour. Res.*, *41*, W04006, doi:10.1029/2004WR003692.

Mulvihill, C. I., B. P. Baldigo, S. J. Miller, D. DeKoskie, and J. DuBois (2009), Bankfull discharge and channel characteristics of streams in New York State, *U.S. Geol. Surv. Scientific Investigations Rep. 2009–5144*.

Nash, D. B. (1994), Effective sediment-transporting discharge from magnitude-frequency analysis, *J. Geol.*, *102*, 79–95.

Newman, M. E. J. (2005), Power laws, Pareto distributions and Zipf's law, *Contemp. Phys.*, *46*, 323–351.

Ogden, F. L., and D. R. Dawdy (2003), Peak discharge scaling in small Hortonian watershed, *J. Hydrol. Eng. 8*(2) 64–73.

Pickup, G., and R. F. Warner (1976), Effects of hydrologic regime on magnitude and frequency of dominant discharge, *J. Hydrol.*, *29*, 51–75.

Pitlick, J. (1994), Relation between peak flows, precipitation, and physiography for 5 mountainous regions in the Western USA, *J. Hydrol.*, *158*, 219–240.

Pitlick, J., and M. M. Van Steeter (1998), Geomorphology and endangered fish habitats of the upper Colorado River 2. Linking sediment transport to habitat maintenance, *Water Resour. Res.*, *34*, 303–316.

Pitlick, J., E. R. Mueller, C. Segura, R. Cress, and M. Torizzo (2008), Relation between flow, surface-layer armoring and sediment transport in

gravel-bed rivers, *Earth Surf. Processes Landforms*, doi: 10.1002/esp.1607 (published online 10/12/07).

Potter, K. W. (2001), A simple method for estimating baseflow at ungaged locations, *J. Am. Water Res. Assoc.*, *37*(1), 177–184.

Press, W. H., S. A. Teukolsky, W. T. Vetterling, and B. P. Flannery (2007), *Numerical Recipes: The Art of Scientific Computing*, 1235 pp., Cambridge Univ. Press, New York.

Rachol, C. M., and K. Boley-Morse (2009), Estimated bankfull discharge for selected Michigan rivers and regional hydraulic geometry curves for estimating bankfull characteristics in southern Michigan rivers, *U.S. Geol. Surv. Sci. Invest. Rep. 2009–5133*.

Richards, K. S. (1982), Rivers: Form and process in alluvial channels, Methuen, London.

Richter, B., J. Kircher, M. Remmer, and B. Forst (1984), Summary of basins and streamflow characteristics for selected basins in Western Colorado, *U.S. Geol. Surv. Open File Rep. 84–137*.

Segura, C. (2008), Effects of sediment transport on benthic organisms in a mountain river, CO, Ph.D thesis, 176 pp., Univ. of Colorado, Boulder, Colo.

Serreze, M. C., M. P. Clark, R. L. Armstrong, D. A. McGinnis, and R. L. Pulwarty (1999), Characteristics of the Western U.S. snowpack from snowpack telemetry (SNOTEL) data, *Water Resour. Res.*, *35*, 2145–2160.

Sherwood, J. M., and C. A. Huitger (2005), Bankfull characteristics of Ohio streams and their relation to peak streamflows, *U.S. Geol. Surv. Sci. Invest. Rep. 2005-5153*.

Surian, N., and E. D. Andrews (1999), Estimation of geomorphologically significant flows in alpine streams of the Rocky Mountains, Colorado (USA), *Reg. Rivers Res. Manage.*, *15*, 273–288.

Torizzo, M., and J. Pitlick (2004), Magnitude-frequency of bed load transport in mountain streams in Colorado, *J. Hydrol.*, *290*, 137–151.

Vogel, R. M., and N. M. Fennessey (1993), L-Moment diagrams should replace product moment diagrams, *Water Resour. Res*, *29*, 1745–1752.

Vogel, R. M., and N. M. Fennessey (1995), Flow duration curves. 2. A review of applications in water-resources planning, *Water Resour. Bull.*, *31*, 1029–1039.

Vogel, R. M., and A. Sankarasubramanian (2000), Spatial scaling properties of annual streamflow in the United States, *Hydrol. Sci. J.*, *45*, 465–476.

Vogel, R. M., J. R. Stedinger, and R. P. Hooper (2003), Discharge indices for water quality loads, *Water Resour. Res.*, *39*(10), 1273, doi:10.1029/2002WR001872.

Whiting, P. J., J. F. Stamm, D. B. Moog, and R. L. Orndorff (1999), Sediment-transporting flows in headwater streams, *Geol. Soc. Am. Bull.*, *111*, 450–466.

Williams, G. P. (1978), Bankfull discharge of rivers, *Water Resour. Res.*, *14*, 1141–1154.

Wolff, C. G., and S. J. Burges (1994), An analysis of the influence of river channel properties in flood frequency, *J. Hydrol.*, *153*, 317–337.

Wolman, M. G., and L. Leopold (1957), River flood plains: Some observations on their formation, *U.S. Geol. Surv. Prof. Pap. 282-C*.

Wolman, M. G., and J. P. Miller (1960), Magnitude and frequency of forces in geomorphic processes, *J. Geol.*, *68*, 54–74.

Woltemade, C. J., and K. E. Potter (1994), A watershed modeling analysis of fluvial geomorphologic influences of flood peak attenuation, *Water Resour. Res.*, *30*, 1933–1942.

J. Pitlick, Department of Geography, University of Colorado at Boulder, Boulder, CO, USA.

C. Segura, Department of Forestry and Environmental Resources, North Carolina State University, Box 8008, Raleigh, NC 27695, USA. (csegura@ncsu.edu)